Manganese-Salen Complexes as Oxygen-Transfer Agents in Catalytic Epoxidations − A Density Functional Study of Mechanistic Aspects

Luigi Cavallo[a] **and Heiko Jacobsen***[b]

Keywords: Density functional calculations / Epoxidation / Manganese / N,O ligands / Radicals

The mechanism of the Jacobsen–Katsuki epoxidation has been investigated by application of density functional theory; the results of a series of calculations for simplified model systems of different spin states are presented. In the chosen computational approach, the epoxidation of ethylene with a cationic five-coordinate model catalyst is predicted to occur through a radical intermediate, similarly to the reaction mechanism calculated for the corresponding neutral six-coordinate species. Although the radical intermediate shows a small energetic preference for the quintet state over the triplet state, the computed reaction profile does not suggest that two-state reactivity involving spin change plays a major role during the oxygen-transfer step. Comparative orbital analysis of the cationic and the neutral complexes elucidates the role of a ligand *trans* to the oxo group. A π-donor *trans* to the forming OR^- ligand in the radical intermediate causes a relative destabilization of a possible quintet occupation, thus conferring spin rigidity to the six-coordinate species derived from the neutral catalyst. A reaction pathway resulting in rotational collapse might involve a spin-crossing process. The ligand framework of the tetra-chelating N,O ligand in the radical intermediate exhibits a considerable amount of ligand folding.

Introduction

Transition metal-catalyzed oxidations play a vital role not only in preparative organic chemistry, but also in biochemical transformations.[1] We mention as one prominent example that manganese is part of the active site in photosystem II,[2] and that the role of metal oxo species in water oxidation and O_2-formation has been convincingly demonstrated.[3,4] For synthetic purposes, cationic Mn^{III}-salen complexes were introduced as effective catalysts for the epoxidation of olefins by Kochi in 1986.[5] Katsuki[6] and Jacobsen[7] designed chiral manganese catalysts, which also allowed for enantioselective epoxidations, by modifying the backbone of the salen ligand. The Jacobsen−Katsuki reaction is currently recognized as one of the most practical methods for the epoxidation of alkenes.[8,9] Jacobsen's catalyst **1** is effective for virtually every class of conjugated olefins, and industrial production of the catalyst on a ton scale has become possible.[10] New developments in catalytic epoxidation with Mn^{III}-salen complexes include the use of ionic liquids, which allow the homogenous chiral catalyst to be immobilized, recovered, and recycled and so enhance the activity of the system.[11]

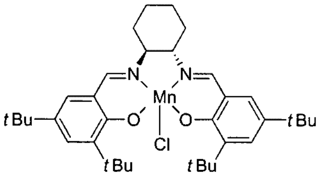

1

The mechanistic scheme commonly proposed for this oxygen-transfer reaction consists of a two-step catalytic cycle (Scheme 1).[8,9,12] Oxygen is transferred from a terminal oxidant to the Mn^{III}-salen catalyst, generating an intermediate Mn^V oxo complex, which in the second step carries the activated oxygen to the olefinic double bond.

The existence of a Mn^V oxo intermediate, first postulated by Kochi and co-workers,[5] was confirmed by electrospray tandem mass spectrometry by Feichtinger and Plattner.[13] In a recent study, these authors used the same technique to elucidate the mechanism of oxygen transfer to the Mn^{III}-salen complex in great detail,[14] identifying a dimeric μ-

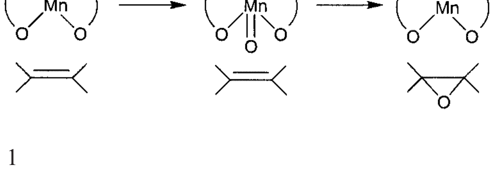

Scheme 1

---

[a] Department of Chemistry, Università di Salerno
Via Salvador Allende, Baronissi (SA) 84081, Italy
[b] KemKom
1864 Burfield Avenue, Ottawa, Ontario, K1J 6T1, Canada
E-mail: jacobsen@kemkom.com
Supporting information for this article is available on the WWW under http://www.eurjic.org or from the author.

oxo-bridged species acting as reservoir species, and for the first time investigating the coordination chemistry of the terminal oxidant iodosylbenzene with regard to the Mn(salen) system. It should be mentioned that related Mn^{V}-oxo complexes have also been detected in solution by Groves and co-workers, who applied rapid-mixing stopped-flow spectrophotometry.[15]

Keenly debated is the second step in the epoxidation reaction, over which a controversy has erupted in the literature (Scheme 2).[16]

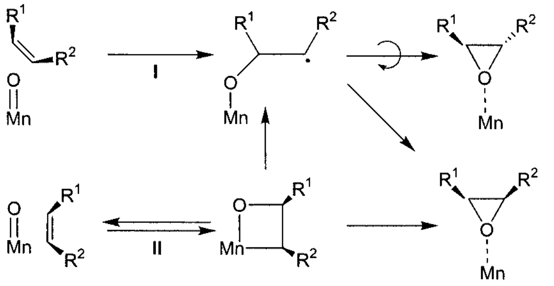

Scheme 2

Since the stereochemistry is determined by the way in which oxygen is delivered to the olefin, detailed knowledge of this step provides the basis for understanding and tuning of the enantioselectivity of the reaction. Both pathway **I**, in which the first attack of the olefin occurs at the oxo center only, and pathway **II**, which proceeds via a manganoxetane, are subjects of discussion. Experimental evidence has been put forward both for the existence of radical intermediates[17] and for the formation of metallacycles.[18] In contrast to direct routes, which should give rise to *cis* epoxides, rotational collapse from the radical intermediate would afford the *trans* product (Scheme 2). This mechanism provides an explanation for the experimentally observed *cis*/*trans* isomerization in the epoxidation of conjugated alkenes.

With regard to the origin of the enantioselectivity, it is generally assumed that it is dominated by steric interactions between the chiral Mn(salen) complex and the two prochiral faces of the olefin. However, it has to be borne in mind that electronic effects, in particular the nature of the substituents in positions 5,5′, also have a strong influence.

Jacobsen developed a mechanistic basis for the electronic effects on enantioselectivity,[19] which assumes the formation of a radical intermediate as the first step in oxygen transfer. Enantioselectivity is tied to the position of the transition state along the reaction coordinate, which can in turn be tuned by electronic variation of the salen ligand system. In connection with the synthesis of optically active α-hydroxy carbonyl compounds, Fell and Adam also showed that the preferentially reacting enantiomer is determined by electronic effects, whereas steric interactions are responsible for the observed stereochemical preference in the double bond epoxidation.[20] When hydroxy group directivity is utilized during the course of the diastereoselective epoxidation,[21] Adam and co-workers conclude that reactions through a metallacycle intermediate and through a direct three-centered transition state both constitute viable reaction mechanisms.[22] Metallacycles have also been discussed by Katsuki and co-workers.[23]

Recently, various density functional (DF) calculations focusing on Mn^{V}-oxo species and their role in olefin epoxidation have appeared. Most of these studies deal with systems **3** or **3⁺**, derived from the Mn^{III}-salen model complexes **2** or **2⁺**, respectively.

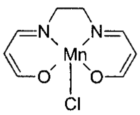

2

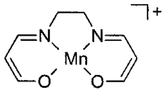

2⁺

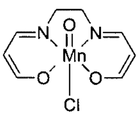

3

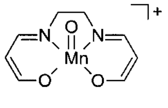

3⁺

Strassner and Houk[24] have reported the results of hybrid-DF[25] calculations with the B3LYP functional[26] on the geometries and multiplicities of the systems described above, and discuss their implications for stereoselectivity. By the same methodology, Svensson and co-workers[27] studied the epoxidation of ethylene with catalyst **3⁺**. They suggest that the reaction begins with alkene attack on the triplet surface, followed by a spin change to the quintet surface, which affords the quintet epoxide product without a barrier. On the triplet surface it was possible to localize a radical intermediate, whereas on the quintet surface the reaction proceeds from the first, very early, transition state directly to the final products without any other intermediates or transition states. The point at which the spin-crossing occurs determines the stereochemistry of the reaction; only if the spin change takes place after the formation of the radical intermediate does *cis-trans* isomerization become possible. The mechanism of the Jacobsen−Katsuki epoxidation is thus explained in terms of two-state reactivity,[28] which has evolved as a new concept in organometallic chemistry.[29] Although reactions that undergo spin inversion have recently been observed in the gas phase,[30] two-state reactivity in the condensed phase has not yet been shown to occur, but "offers a conceptually attractive explanation for these experimental findings that are difficult to understand by any other existing concepts."[29]

We have investigated a similar reaction profile for olefin epoxidation with catalyst **3**,[31] by applying BP86 DF calculations.[32] Contrary to the results obtained by Svensson and co-workers, our calculations for the reaction profile for ethylene epoxidation with **3** indicate that the reaction occurs on the triplet surface, and is likely to involve radical intermediates. The reaction profile on the quintet surface, for which both a radical intermediate and transition states for C−O bond formation could be localized, is generally higher in energy than that of the triplet surface, and spin inversion does not seem to be a likely process. Both studies on system **3** and **3**$^+$, however, concur on the fact that formation of a metallacycle during the epoxidation is not likely to occur.

One of the differences between the two mechanistic models described above is the presence of a free coordination site versus an occupied one *trans* to the oxo group. The coordination chemistry of Mn salen complexes and effects of axial ligation have recently been investigated by electrospray tandem mass spectrometry in combination with hybrid DF calculations.[33] This study shows that the presence of a *trans* ligand has a significant influence not only on the coordination geometry of the salen framework, but also on the relative energies of different spin states. Similar observations have also been made by Strassner and Houk.[24]

A further difference between our previous study and the contribution by Svensson and co-workers is the choice of computational methodology. Although it has been convincingly demonstrated that DF theory in general constitutes a powerful tool for the prediction of structures and energetics in transition metal chemistry[34] with an accuracy of the gradient corrected method similar to, or better than, standard correlated methods,[35] systematic studies investigating the performance of different functionals for certain problems in transition metal chemistry have only recently begun to appear.[36,37] When it comes to manganese complexes related to the problem at hand, successful applications both of the B3LYP[38] and of the BP86[39] functionals have been demonstrated in the literature. However, it was recently shown by high-level ab initio calculations [coupled cluster CCSD(T)] that a computational procedure based on the BP86 density functional generates numerical results significantly more reliable than those obtained by a B3LYP approach for the Mn-catalyzed epoxidation reactions.[40]

Given the importance of the Jacobsen−Katsuki epoxidation, we decided to reinvestigate the oxidation of ethylene with catalyst **2**$^+$ by means of BP86-DF calculations. This study complements our previous investigations on the corresponding neutral system **2**.[31] Comparison between the energy profiles for the neutral and cationic active species should allow insights on the role of the axial ligand to be obtained. Questions to be addressed include the existence of possible oxametallacyclic intermediates, as well as a possible precoordination of the olefinic double bond. Furthermore, the coordination geometry of the tetra-chelating N,O ligand is investigated, and the possibility of spin inversion is discussed in connection with the geometries of radical intermediates and of transition states. Moreover, since there are some discrepancies between the chemical pictures obtained by the different DF approaches, we believe it is also worthwhile to investigate the energy profile for the cationic system **2**$^+$ with the BP86 functional. We believe that a critical comparison between different computational approaches should allow further details on the mechanism of this relevant reaction to be gained.

Results and Discussion

Electronic Structures of Mn(salen) Model Compounds: (Supporting information including optimized geometries and final bonding energies available, see also footnote on the first page of this article).The qualitative molecular orbital diagram for a d^4-ML$_4$ complex[41] suggests that, for the square planar compound **2**$^+$, triplet and quintet configurations − corresponding to total spin density values of 2α, *S2*, and 4α, *S4*, respectively − have to be considered. Our nomenclature was chosen to reflect the spin density, and should not be mistaken with spin states or $<S^2>$ values. We calculated an energetic difference of 67 kJ/mol, in favor of the quintet state, between the *S2* and *S4* geometries in **2**$^+$. A singlet ground state can be achieved if the metal d orbitals adopt the familiar two-below-three pattern of a tetrahedral ligand field. The *S0*−**2**$^+$ molecule, however, which is consequently strongly distorted toward a tetrahedral geometry, is 147 kJ/mol higher in energy than *S4*−**2**$^+$. This coordination mode of the core ligand is not considered any further. Complex **2**$^+$ thus possesses an electronic structure similar to that of **2**, for which the energetic difference between the *S4* and *S2* geometries amounts to 38 kJ/mol,[31] *S4*−**2** again being more stable. These results are in agreement with EPR spectroscopic studies of the Mn(salen) complex **1** in CH_2Cl_2 at 77 K performed by Talsi and co-workers,[42] which reveal the presence of manganese species with spin states S = 2. Recent EPR studies by Campbell and co-workers[43] confirm these findings.

For the active species involved in oxygen transfer, the cationic Mn^V complex **3**$^+$, we calculate the *S0* state to be most stable, with a triplet *S2*−**3**$^+$ 27 kJ/mol higher in energy, and a quintet *S4*−**3**$^+$ 101 kJ/mol less stable than the ground state. For the corresponding hexacoordinate compound **3**, on the other hand, the two states *S0* and *S2* are at virtually the same energy level, with a marginal preference for the singlet. In addition, the quintet state *S4*−**3** is only 45 kJ/mol higher in energy than the *S0* local minimum geometry. The molecular orbital diagram for the Mn^V-oxo species **3** and **3**$^+$, presented in Figure 1, offers an explanation for this observation.

The energy level schemes are derived from the corresponding singlet geometries. For **3**$^+$, the HOMO is dominated by contributions from a Mn-d$_{x^2-y^2}$ orbital, whereas the LUMO and LUMO+1 are metal-based, derived from the orbitals d$_{xz}$ and d$_{yz}$. However, the last two orbitals are strongly antibonding with respect to the p orbitals of the oxo ligand. They are therefore raised in energy relative to the HOMO, and the resulting rather large HOMO/LUMO gap energetically stabilizes the singlet state. The degeneracy of the LUMO and LUMO+1 is lifted, due to orbital contributions from the tetra-chelating ligand. For the HOMO of **3**, we have substantial antibonding interaction between the Mn-d$_{x^2-y^2}$ orbital and occupied p orbitals of the Cl$^-$ ligand. This interaction causes an energetic destabilization of the HOMO. As a consequence, the HOMO/LUMO gap is lowered, in favor of a triplet configuration. This orbital interaction provides a first hint as to how an additional π-

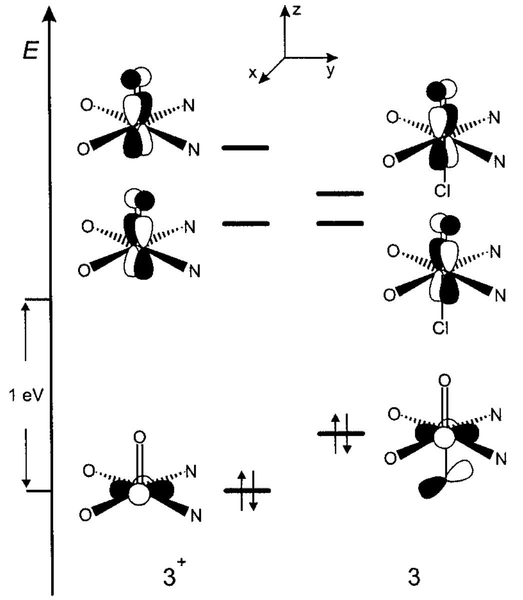

Figure 1. Frontier orbital diagram for Mn^V oxo complexes $\mathbf{3}^+$ and **3**

donor *trans* to the oxo ligand might exert an influence on the oxygen-transfer process.

Table 1 compares the relative energies of different spin state geometries of $\mathbf{2}^+$, **2**, $\mathbf{3}^+$, and **3** with the results of the two B3LYP studies by Strassner and Houk[24] and by Svensson and co-workers,[27] as well as with the recent study of Abashkin and co-workers.[40] This comparison focuses on technical aspects of the calculations, and the results in Table 1 are organized according to basis set quality into three groups. Group **I** refers to calculation utilizing a triple-ζ basis for Mn, and a double-ζ basis plus polarization for the remaining atoms. In group **II**, a double-ζ basis is used and polarization functions are added for Mn, Cl, O, and N, whereas group **III** essentially refers to double-ζ basis set calculations.

Table 1. Relative energies (kJ/mol)[a] of complexes $\mathbf{2}^+$, **2**, $\mathbf{3}^+$, **3** for different spin densities

[a]		$\mathbf{2}^+$		**2**		$\mathbf{3}^+$			**3**		
		S2	*S4*	*S2*	*S4*	*S0*	*S2*	*S4*	*S0*	*S2*	*S4*
I	BP86[b]	67	0	38	0	0	27	101	0	1	45
	B3LYP[c]	113	0	82	0	0	15	47	43	0	8
II	BP86d.	–	–	–	–	0	53	141	0	25	72
	B3LYP[d]	–	–	–	–	–	–	–	39	5	0
III	B3LYP[e]	–	–	–	–	7	0	21	–	–	–
	B3LYP[f]	–	–	–	–	6	0	11	–	–	–

[a] Literature values have been converted. [b] Values for **2** and **3** from ref.[31] [c] 6−31G* (HCNOCl)/TZ(Mn) basis, ref.[24] [d] DZVP basis for Mn, Cl, N O, DZ basis for C, H; ref.[40] [e] DZ basis, ref.[40] [f] (14s,11p,6d) primitive basis augmented by two p and one diffuse d function contracted to [6s,5p,3d] for Mn, DZ basis for ligands, ref.[27]

Referring to group **I**, for the two cationic species and for **2,** our calculations are in qualitative agreement with the data reported by Strassner and Houk.[24] In particular, both sets of calculations predict the same energetic ranking for the Mn^{III} and Mn^V species, and indicate that the addition of the π-donating Cl^- ligand reduces the energy gap between the *S2* and *S4* states by about 30 kJ/mol. The reason is again to be found in the antibonding contributions from p orbitals of the Cl^- ligand, which destabilize only three of the four singly occupied metal d orbitals, rendering triplet occupation more stable for **2** than for $\mathbf{2}^+$. One difference between the BP86 and B3LYP functionals is the fact that the hybrid method, which contains an admixture of pure Hartree−Fock exchange, energetically favors the *S4* spin states. Thus, in cases in which *S4* is the ground state, such as **2** and $\mathbf{2}^+$, the energy difference between the *S4* and *S2* geometries is higher, by about 45 kJ/mol, for the B3LYP calculation than for BP86 results. On the other hand and for the same reason, *S4*−$\mathbf{3}^+$ is energetically more disfavored in the BP86 calculation, by 54 kJ/mol.

A major discrepancy is found for compound **3**. As discussed above, the BP86 calculations predict a singlet and a triplet geometry at almost the same energy. In contrast, the B3LYP method results in a triplet ground state, with the quintet close by in energy, and the singlet significantly higher.

A reason for this discrepancy may be found if group **II** data are included in the discussion. For $\mathbf{3}^+$ and **3** we find that the results of the BP86 calculations of Abashkin and co-workers[40] follow the same qualitative trend as our current and previous results. However, the energy differences between different spin states are significantly different. For **3** in particular, Abashkin and co-workers predict a singlet state, clearly favored over a triplet state, as ground state, whereas our calculations indicated that a singlet and a triplet state are essentially at the same energy level, well separated from a quintet state. This might be a first indication of the importance of an extended basis set for calculations on the type of molecules under investigation, describing the metal center on a triple-ζ basis, and including polarization functions for all atoms. Comparing B3LYP calculations of group **I** and **II**, we again find qualitative agreement. Triplet and quintet states are close in energy, whereas the singlet state is significantly higher in energy. However, Strassner and Houk find a triplet state at lowest energy, the quintet being 8 kJ/mol higher, whereas Abashkin and co-workers find the triplet to be 5 kJ/mol higher than the quintet, the latter now being the ground state. This again might be an indication for significant basis set influences.

Abashkin and co-workers have also addressed the comparison between the BP86 and the B3LYP approaches.[40] We recall that for **3** the two approaches provide qualitatively different results, the relative energy rankings being $S0 \approx S2 < S4$ for BP86 and $S0 > S2 \approx S4$ for B3LYP. In addition to DFT calculations, Abashkin and co-workers performed high level ab initio calculations, and the results for **3**, obtained from coupled cluster CCSD(T) calculations, are in line with BP86, but not with B3LYP. This study suggests that for this type of molecules the pure BP86 functional provides a more appropriate and a more suitable approach than the popular B3LYP hybrid functional.

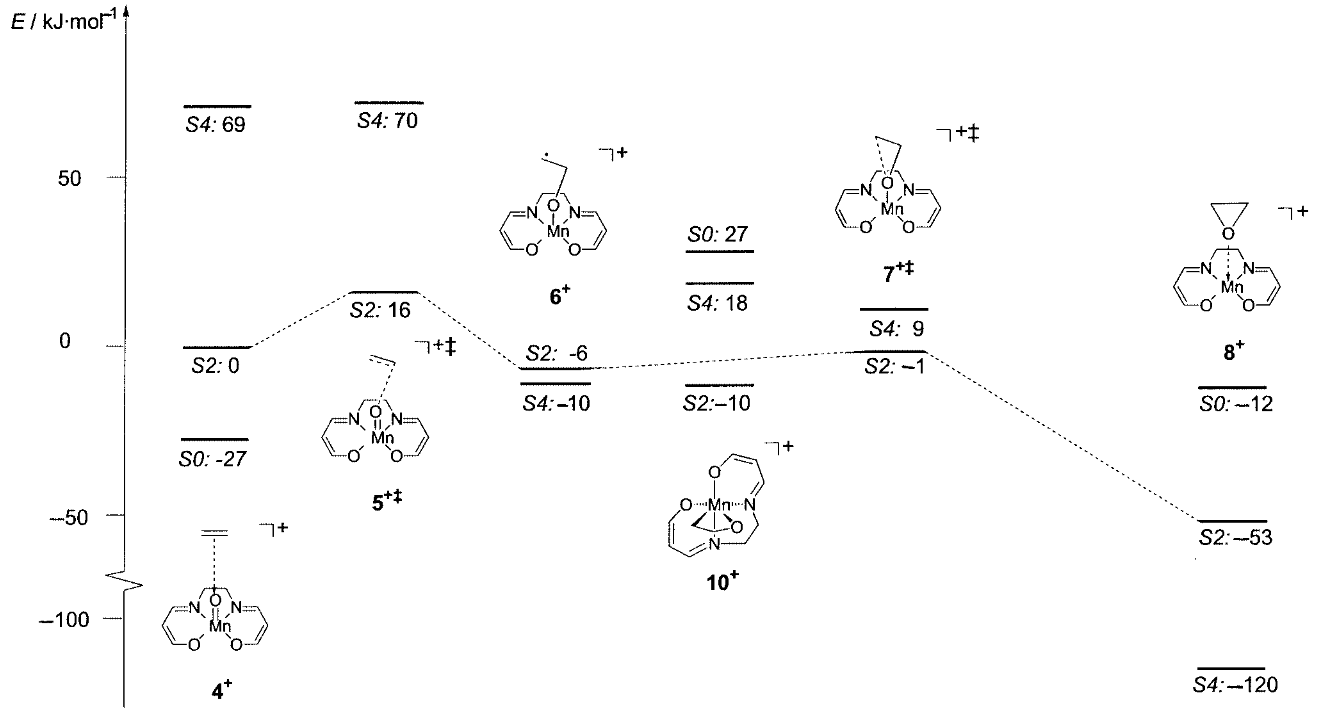

Figure 2. Energy profile for the epoxidation reaction

Finally, turning to group **III**, we find that the two sets of B3LYP calculations are in good qualitative agreement. However, B3LYP calculations without inclusion of polarization functions are significantly different from the B3LYP result for group **I**. This comparison again underlines the importance of an extended basis set for calculations on the type of molecules under investigation.

The importance of basis sets is further evident when the DZVP-BP86 results of Abashkin and co-workers for complex **2** are considered. The authors find a triplet state at lowest energy, a quintet state being 5 kJ/mol higher, whereas our previous BP86 results report the triplet as 38 kJ/mol above the quintet.

The Reaction Profile for Oxygen Transfer: The calculated energy profile for epoxide formation with the model catalyst $\mathbf{3}^+$ is displayed in Figure 2.

Relative energies for reactants, intermediates, transition states, and final products are reported for the *S0*, *S2*, and *S4* energy hypersurfaces. We comment on each of the single steps in more detail below.

The Reference System $\mathbf{4}^+$: In our reference system, the incoming olefin approaches the manganese catalyst from the site of the oxo ligand, and forms a weakly bonded adduct. In this complex, the distances between the olefinic C atoms and the Mn=O function amount to 300 and 320 pm, respectively. The system *S2*−$\mathbf{4}^+$ is set at 0 kJ/mol on the energy scale, and the energies of all other species are then given relative to *S2*−$\mathbf{4}^+$. It is worth mentioning that the relative energies of the different spin states *S0*, *S2*, and *S4* are in essence identical to those obtained for the free oxo cation $\mathbf{3}^+$ (compare Table 1). We chose this aggregate as reference state over the completely separated molecules (C_2H_4 + $\mathbf{3}^+$), since some of the computational errors involved in determining the energetics of bond-forming reactions, especially those stemming from basis set superposition effects,[44] are reduced in such a combined approach.

The First Transition State $\mathbf{5}^{+\ddagger}$: On the *S2* energy hypersurface, the energy of the $\mathbf{5}^{+\ddagger}$ structure lies 16 kJ/mol above the reference state *S2*−$\mathbf{4}^+$, indicating that the first C−O bond formation does not represent much of an energetic barrier. The distance $d_{\mathrm{C-O}}$ amounts to 189 pm, similar to that calculated for the corresponding structure *S2*−$\mathbf{5}^{\ddagger}$.[31] The Mn−O bond is 169 pm, significantly elongated compared to that in *S2*−$\mathbf{3}^+$ ($d_{\mathrm{Mn-O}}$ = 161 pm). The values of spin density at the Mn center and the terminal C atom of the olefinic substrate amount to 2.4 α and 0.5 β, respectively, indicating that the epoxidation reaction is initialized by a one-electron reduction process. From both the electronic and the geometric structures of *S2*−$\mathbf{5}^{+\ddagger}$ it can be concluded that *S2*−$\mathbf{5}^{+\ddagger}$ has to be classified as a late, or product-like, transition state on the triplet surface. This observation, together with an orbital analysis for the radical intermediate presented in the next section, also rules out the existence of an energetically low-lying *S0*−$\mathbf{5}^{+\ddagger}$ geometry. A different situation is found when the process is assumed to take place on the quintet surface. The *S4*−$\mathbf{5}^{+\ddagger}$ state is already reached when the bond-forming C-atom is about 240 pm away from the oxo center, and is only marginally higher in energy than *S4*−$\mathbf{4}^+$. Also, the electronic situation more closely resembles that of the reactant system, with spin density mostly located at the metal center and at the oxo ligand. In this case the reaction occurs through an early transition state, as already noted by Svensson and coworkers.[27]

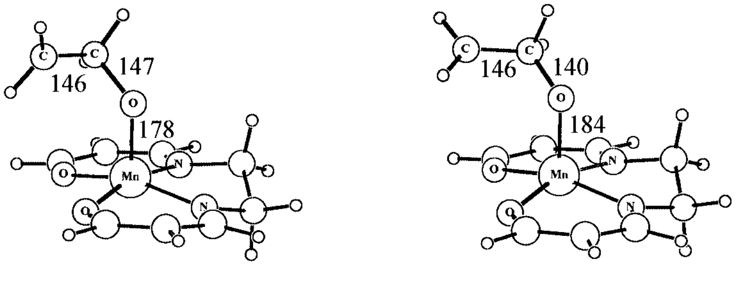

S2-**6**$^+$: 4 kJ/mol S4-**6**$^+$: 0 kJ/mol

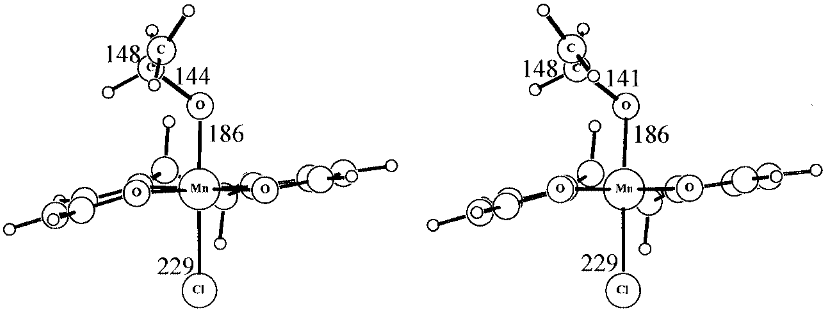

S2-**6**: 0 kJ/mol S4-**6**: 9 kJ/mol

Figure 3. Optimized structures and relative energies for *S2* and *S4* geometries of **6**$^+$ and **6**

The Radical Intermediate 6$^+$: Figure 3 compares the geometries and relative energies of the radical intermediates *S2*−**6**$^+$ and *S4*−**6**$^+$ with those of the corresponding neutral systems *S2*−**6** and *S4*−**6**.

A few important differences deserve more detailed discussion. Firstly, we note that the Mn−O distances in the cationic systems are between 8 and 2 pm shorter than those found for the system with the Cl ligand *trans* to the oxo group, pointing to a *trans* influence of the additional π-donor ligand. We also see that both chloro species *S2*−**6** and *S4*−**6** have the same Mn−O separation, whereas the triplet geometry shows significantly shorter Mn−O distances for the cationic complexes **6**$^+$. Secondly, we observe that the coordination geometry of the quintet species is substantially different from that of the triplet systems. In the latter, the original orientation of the olefin is preserved, whereas in the former we see that the terminal CH_2 group is rotated by 90°. Thirdly, for the cationic system **6**$^+$ we calculate a small energetic preference for the *S4* state (of 4 kJ/mol), whereas for the neutral system **6** the *S2* state is more stable by 9 kJ/mol.

A qualitative analysis of the frontier Kohn-Sham orbitals corresponding to the α spin density for the *S2* geometries provides a rationale for the above observations. The highest occupied orbital 1a and the lowest unoccupied orbitals 2a for system **6**$^+$ and **6** are presented in Figure 4.

For the formal Mn^{IV} species, these orbitals are mainly Mn-based d orbitals, undergoing antibonding interaction with the $-OC_2H_5$ ligand. For **6**, we see that the interplay of the p-Cl and d-Mn orbitals adds additional antibonding character. A promotion of one electron into orbital 2a, resulting in an electronic quintet state, is thus disfavored for **6** by an increase in the repulsive Mn−Cl interaction. This argument suggests that the role of the π-donor in the *trans* position is a relative destabilization of a possible quintet occupation, thus conferring spin rigidity to the six-coordinate species derived from the neutral catalyst **2**. In our previous study we calculated that *S2*−**6** is energetically favored over *S4*−**6** by 9 kJ/mol. We also see that the orbital 2a has large contributions from the p orbitals of the terminal CH_2 group, which interact with the formerly oxo ligand in an antibonding fashion. As a consequence, when this molecular orbital becomes occupied, the terminal CH_2 group twists to relieve this destabilizing interaction. As mentioned before, the *S4* geometries both for **6** and for **6**$^+$ do indeed exhibit this structural characteristic.

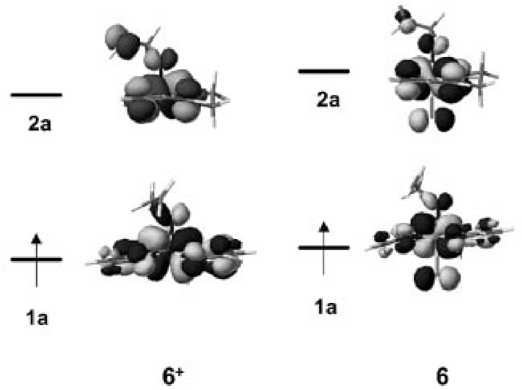

Figure 4. Frontier orbitals for the Mn^{IV} complexes **6**$^+$ and **6**

Another important feature observed in Figure 3 is the folded geometry of the tetra-chelating N,O ligand. This arrangement has been identified as one of the key points in the mechanism of enantioselectivity[45] and we return to a more detailed analysis of this structural feature at a later point.

The Second Transition State $7^{+\ddagger}$: On the *S2* surface, the transition state $7^{+\ddagger}$ for the formation of the second C−O bond is only 9 kJ/mol higher in energy than the triplet intermediate (Figure 2). The long length of the newly forming C−O bond classifies *S2*−$7^{+\ddagger}$ as an early transition state. Product formation from the radical intermediate thus occurs without much of an energetic barrier. In comparison with *S2*−$7^{+\ddagger}$, the transition state *S4*−$7^{+\ddagger}$ is 10 kJ/mol higher in energy. The characteristic mode receives a strong contribution from the CH_2-twist required for ring closure to form the epoxide.

The Epoxide Adduct 8^+: Characteristic bond lengths and bonding energies for epoxide complexes 8^+ are compiled in Table 2.

Table 2. Bond lengths (pm) and bond energies (kJ/mol) for Mn^{III} epoxide complexes 8^+

	d_{Mn-O}	BE
S0−8^+	198	123
S2−8^+	199	85
S4−8^+	223	85

We see that the forming epoxide is only loosely bound to the metal centers, the coordination geometries and relative energies of which resemble those of the Mn^{III} precursor models 2^+. Only the *S0* complex is somewhat more strongly stabilized, relative to the *S2* and *S4* systems. The most stable complex is therefore *S4*−8^+, followed by *S2*−8^+, 67 kJ/mol higher in energy. If the cationic complexes considered here are the true catalytically active species, a spin change during the course of the epoxidation reaction might indeed occur in the reaction sequence. On the other hand, it is worth mentioning that the energetic difference between the corresponding chloro complexes *S4*−**8** and *S2*−**8** only amounts to 4 kJ/mol, in favor of the quintet state.[31] As we have already argued in this context, catalytic cycles based on Mn complexes derived from the hexacoordinate model system **3** are likely to take place as spin-conserving reactions.

As mentioned before, the resulting epoxides are only loosely bonded to the metal center. Furthermore, we should keep in mind that our calculations are performed on isolated systems in the gas phase, and we can expect that solvent effects should substantially stabilize the coordinatively unsaturated cation 2^+, thus further reducing the bond energy of the epoxide ligand. If in addition we take into account unfavorable coordination entropy, for which at room temperature a $T\Delta S$ contribution between 40 and 50 kJ/mol can be estimated,[46] we conclude that product liberation is not a critical step in the catalytic cycle.

The Transition State $9^{+\ddagger}$ for Synchronous Attack: So far, we have considered the epoxidation reaction as a sequence of two consecutive C−O bond-formation steps. Alternatively, one might think of a concerted mechanism that involves an epoxide-like transition state $9^{+\ddagger}$ (Scheme 3).

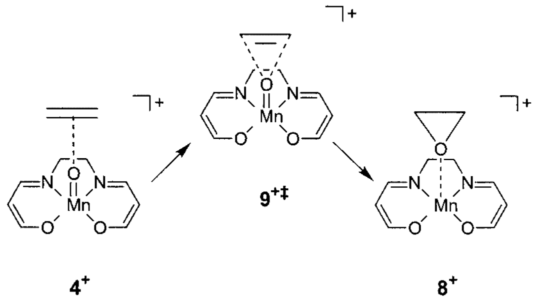

Scheme 3

Such a mechanism, however, although consistent with certain experimental findings,[22] does not offer a simple explanation for the observed *cis*/*trans* isomerization that frequently occurs in the epoxidation reaction. For our model reaction we have localized the corresponding structures both on the triplet and on the quintet surfaces. Compared to the reference system, structures *S2*−$9^{+\ddagger}$ and *S4*−$9^{+\ddagger}$ are 32 and 74 kJ/mol higher in energy, respectively. This implies that, on the *S2* surface, the concerted mechanism is kinetically disfavored relative to the stepwise reaction by 16 kJ/mol. Even in the *S4* case the stepwise reaction is favored by 4 kJ/mol.

Ligand Folding: As noted above in the context of the radical intermediate 6^+, the tetra-chelating N,O model ligand shows significant deviations from a planar structure, and has a folded geometry, as shown in Figure 3. We now discuss ligand folding for the representative geometries of the oxomanganese species 3^+ and **3**, as well as of the radical intermediates 6^+ and **6**, including the corresponding structures **3s** and **6s** of a Mn(salen) complex.[31]

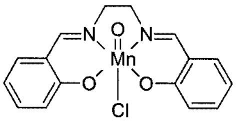

3s

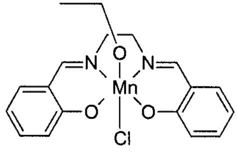

6s

Ligand folding is discussed in connection with the bent angles φ_{up} and φ_{down}, and the distance of pyramidalization, d_P. A bent angle φ is defined as $\varphi = 180° - \angle(Mn-X_{NO}-X_R)$, the angle $\angle(Mn-X_{NO}-X_R)$ being that measured between the metal center, the midpoint of adjacent N,O heteroatoms (X_{NO}), and the midpoint of the sixmembered ring containing the metal and the N,O heteroatoms (X_R, Scheme 4).

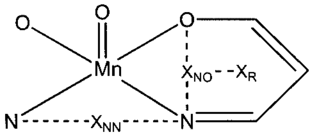

Scheme 4

The angle φ_{up} indicates the part of the tetra-chelating N,O ligand being bent towards the oxo or towards the ethoxy ligand, whereas φ_{down} characterizes the part of the tetra-chelating N,O ligand bent towards the free coordination site or towards the chlorine ligand. Furthermore, the distance of pyramidalization d_P is defined as the separation between the metal atom and the $O-X_{NN}-O$ plane, X_{NN} being the midpoint between the two N atoms. A value of d_P close to zero indicates that the metal essentially lies within the O,N,N,O coordination plane. The values for the folding angles and for the distance d_P are collected in Table 3.

Table 3. Relevant angles (°) φ_{up}, φ_{down} and distance of pyramidalization (pm) d_P for cationic (this work) and neutral (from data of ref.[31]) Mn complexes

	S2			S4		
	φ_{up}	φ_{down}	d_P	φ_{up}	φ_{down}	d_P
$\mathbf{3}^+$	18	8	42	7	2	22
3	19	17	11	3	13	4
3s	10	16	0	10	17	1
$\mathbf{6}^+$	20	5	29	18	3	31
6	8	16	0	8	15	0
6s	8	15	0	8	15	0

The folded ligand geometries as shown in Figure 3 are characterized by bent angles φ being 10° or larger, and by d_P being essentially zero. Inspection of the values reported in Table 3 indicates that highly bent angles φ are found in all cases, with the single exception of *S4*$-\mathbf{3}^+$. For the cationic molecules, however, the metal atom is considerably shifted out of the O,N,N,O coordination plane with values of d_P of between 20 and 45 pm. The cationic molecules do not display the folded geometry as shown in Figure 3, and they probably also do not posses the ability to form a chiral pocket, needed for transfer of enantioselectivity.[45] On the other hand, the neutral systems under consideration display φ and d_P values indicative of a folded ligand geometry. In particular, we note that similar structures are observed for the salen ligand in the radical intermediate **6s** and for the model ligand in complex **6**. It has recently been suggested that the degree of ligand folding is determined by the nature of the axial ligand in Mn(salen) complexes, which in turn has implications for the reaction rate of epoxidation reactions.[47]

Structural Alternatives: We briefly discuss two further complex geometries that might be of importance: namely a metallacycle $\mathbf{10}^+$ and an olefin complex of the Mn^V-oxo species, $\mathbf{11}^+$. Representative structures are displayed in Figure 5.

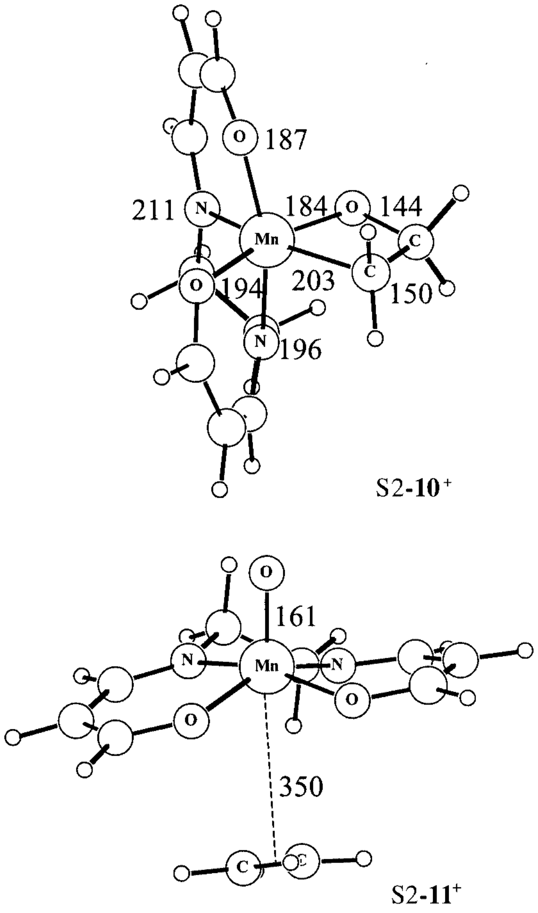

Figure 5. Representative *S2* geometries for a possible manganaoxetane $\mathbf{10}^+$ (above), and an Mn^V-oxo olefin adduct $\mathbf{11}^+$ (below)

Metallacyclic Intermediates: The possibility that metallacycles might be viable intermediates in the epoxidation reaction, and might play a key role in the mechanism of enantioselectivity, has been the subject of a vivid debate in the literature.[17] Indeed, one of the first models of the chirality transfer deduced from calculations uses a manganoxetane as a key intermediate.[48] We have already mentioned that the orbital analysis for structures $\mathbf{6}^+$ points to the possible existence of metallacyclic intermediates. We were able to locate local minima corresponding to such a species on the *S0*, *S2*, and *S4* hypersurfaces, their relative energies being given in Figure 2. Interestingly, the structure *S2*$-\mathbf{10}^+$ is energetically even slightly more stable than the radical intermediate. Its geometry is displayed in Figure 5. The Mn$-$O distance of the four-membered ring is about 6 pm longer than *S2*$-\mathbf{6}^+$, but still within the calculated range for other Mn$-$O bonds. The Mn$-$C bond is 203 pm long, substantially shorter than the Mn$-$C separations in the radical intermediates (around 230 pm). The Mn center possesses a pseudo-octahedral coordination geometry, with a significantly elongated Mn$-$N bond *trans* to the oxacycle. The formation of the oxacycle is favored since the Mn center in $\mathbf{6}^+$ is coordinatively unsaturated. Indeed, a seven-coordinated manganaoxetane **10** is 104 kJ/mol higher in energy than the radical intermediate **6**.[31] Although structure $\mathbf{10}^+$ might be an alternative for an intermediate local minimum geometry, it is not likely to play a major role in product formation. We calculated that formation of $\mathbf{8}^+$ starting from $\mathbf{10}^+$, rather than $\mathbf{6}^+$, is associated with an activation barrier of about 35 kJ/mol. This result is in agreement with a recent study that made use of electrospray ionization in combination with tandem mass spectrometric techniques.[49] It was found that the presence of axial ligands decreases the stability and thus enhances the reactivity of the Mn=O moiety. In the cationic system, the manganaoxetane $\mathbf{10}^+$ is an energetically favorable intermediate in comparison with the radical intermediate $\mathbf{6}^+$, but possesses a higher activation barrier towards product formation, and thus a reduced reactivity. In contrast, systems with axial ligands do not possess energetically favorable, metallacyclic resting intermediates.[31]

Olefin Pre-Coordination: Since the catalytic model system $\mathbf{3}^+$ is coordinatively unsaturated, one might consider the possibility that the olefinic substrate coordinates to the metal center before the oxygen transfer occurs. We investigated possible complexes of this type on the S0, *S2*, and *S4* surfaces, and found in all cases that the olefin is only weakly bound. A representative geometry *S2*−$\mathbf{11}^+$ is shown in Figure 5. The distance between the olefin and the metal center amounts to about 350 pm, and the relative energy is only 4 kJ/mol lower than the one calculated for the reference system *S2*−$\mathbf{4}^+$. The pre-coordination of an olefin can thus be excluded as a vital step in the epoxidation reaction. This conclusion is in agreement with the results of the recent electrospray tandem mass spectrometric study by Plattner and co-workers, who, in a suitable experimental set-up, did not find any indication of pre-coordination of the substrate as prerequisite for oxidation.[33]

Comparison with $\mathbf{d^0}$ Metal Oxo and Peroxo Species: In this final section we present a brief comparison with related theoretical work on oxygen-transfer reactions involving transition metal complexes. Olefin epoxidations mediated by transition metal oxo complexes in high oxidation states, especially those catalyzed by Herrmann-type complexes $[ReO(O_2)_2CH_3]$ and Mimoun-type complexes $[MoO(O_2)_2(OPR_3)]$, have recently generated much interest among experimentalists and theoreticians alike, and Rösch's[50] and Deubel and Frenking's[51] groups have presented detailed theoretical mechanistic studies. The interested reader will also find extensive references to the literature in these computational contributions. Unlike in this work, the olefin attacks an oxygen center in a *concerted* fashion. The preferred site of initial attack is a peroxo ligand, giving rise to *spiro* oxygen in the transition state. Using charge decomposition analysis, Deubel and Frenking[51a] have characterized the electronic nature of the initial attack in terms of classical donor-acceptor interactions, in which the d^0 metal oxo and peroxo species attack the olefin in an electrophilic manner. For the Mn(salen) systems, charge analysis based on Voronoi deformation densities suggests a similar electronic picture. However, the characteristic feature of the transition states $\mathbf{5}^+$ and **5** is a build-up of spin density at the terminal carbon atom. This process is essentially responsible for the locally asymmetric attack of the olefin at the oxo center, which further determines the geometric features of the transition state necessary for chirality transfer.[45] Consistently with our findings, Deubel and Frenking conclude that olefin precoordination at the metal center does not apparently play a role in Mo^{IV}-catalyzed epoxidation reactions,[51c] the reaction profile in both cases being determined by direct oxygen attack of the olefin.

Conclusion

The main results of this study are summarized in the following points. By our computational approach, the epoxidation of ethylene with the cationic five-coordinate model catalyst $\mathbf{3}^+$ is predicted to occur through a radical intermediate, similarly to the reaction mechanism calculated for the corresponding neutral six-coordinate species **3**. In contrast to the reaction profile for **3**, we do not find a clear preference for the *S2* state throughout the whole process. The radical intermediate $\mathbf{6}^+$ shows a small energetic preference for the quintet state over the triplet state. However, contrary to previous studies,[27] we were able to locate a radical intermediate as a local minimum structure on the *S4* hypersurface. On inspection of the computed reaction profile, it seems unlikely that two-state reactivity involving spin change might play a major role in the oxygen-transfer step. Comparative orbital analysis of the cationic and the neutral complexes provides an explanation as to how the ligand *trans* to the oxo group confers spin rigidity to the catalytic systems. However, the different coordination geometries of models $\mathbf{6}^+$ and **6** on the *S2* and *S4* surfaces, respectively, indicate that spin change might indeed be of importance to epoxide formation. Whereas in the *S2* species the two carbon centers of the olefinic substrate are still in π-conjugation, the terminal methylene group in the *S4* complexes is rotated by 90°. This points to the possibility that the pathway of rotational collapse might involve a spin-crossing process. Metallacyclic intermediates might occur during the epoxidation reaction mediated by cationic complexes. However, these complexes constitute resting states, and are likely to display a reduced reactivity towards epoxide formation, in comparison with radical intermediates. Pre-coordination of an olefin is likely to be excluded as a vital step in the epoxidation reaction

This and our previous studies[31] strongly suggest that the crucial step to enantioselectivity is the transition state of the first carbon-oxygen formation. From this assumption, and from the results obtained so far, we have already developed a model that explains the enantioselectivity in the Mn(salen)-catalyzed epoxidation of olefins.[9,19,45] Nevertheless, one has to keep in mind the fact that solvent effects as well as the presence of auxiliary ligands are likely to influence the course of the epoxidation reaction. In addition, reaction profiles in which other Mn^{IV} species are involved in the epoxidation reaction have recently been addressed in the literature,[52] and deserve further computational attention. Recent theoretical studies[53] have demonstrated a general interest in mechanistic aspects of transition metal-mediated reactions resulting in the formation of three-membered ring systems, and recent experimental work[54,55] illustrates the ongoing discussion of the mechanistic aspects of enantioselective epoxidation reactions. In particular, the contribution by Adam and co-workers experimentally addresses the question of whether radical or cationic intermediates are present in the Mn(salen)-catalyzed epoxidation, and attributes counterion effects to computationally assessed ligand-dependent reaction profiles.[55] It is to be hoped that this study will prove to be helpful in supporting such studies, and will provide further impetus for future work, experimentally as well as theoretically.

Computational Details

Spin-polarized calculations were performed with the ADF program package, version 2.3.0.[56] The local exchange-correlation potential of Vosko and co-workers[57] was augmented self-consistently by Becke's exchange gradient-correction and Perdew's correlation gradient-correction (BP86).[32] The ADF basis set IV (triple-ζ STO plus one additional $4p$ function) was used for Mn, whereas basis set III (double-ζ STO plus one polarization function) was employed for the remaining atoms. These basis sets imply the use of the frozen core approximation, in which only the n- and $(n + 1)$-valence orbitals are treated explicitly in a self-consistent manner.[58] The numerical integration scheme developed by te Velde[59] was used, and the grid was chosen such that representative test integrals were evaluated with an accuracy of at least four significant digits. Analytical gradients were calculated by the method described by Versluis.[60] Transition states were first traced by a synchronous linear transit method, and then refined by establishing one negative frequency in the spectrum of the approximate Hessian used to construct geometry updates. The validity of this approach has been demonstrated in the literature.[61]

Acknowledgments

Support from the Italian MURST (L.C.), and access to the computational facilities of the Rechenzentrum der Universität Zürich (H.J.) are gratefully acknowledged. L.C. thanks the CIMCF of the Università Federico II of Napoli for technical support. The constructive comments of one of our referees are highly appreciated.

---

[1] All articles in, *Struct. Bond.* **2000**, *97*.

[2] [2a] R. J. Debus, *Biochim. Biophys. Acta* **1992**, *1102*, 269–352. [2b] V. K. Yachandra, K. Sauer, M. P. Klein, *Chem. Rev.* **1996**, *96*, 2927–2950.

[3] J. Limburg, J. S. Vrettos, L. M. Liable-Sands, A. L. Rheingold, R. H. Crabtree, G. W. Brudvig, *Science* **1999**, *108*, 1524–1527.

[4] [4a] M. R. A. Blomberg, P. E. M. Siegbahn, S. Styring, G. T. Babcock, B. Åckermark, P. Korall, *J. Am. Chem. Soc.* **1997**, *119*, 8285–8292. [4b] P. E. M. Siegbahn, *Inorg. Chem.* **2000**, *39*, 2923–2935.

[5] K. Srinivasan, P. Michaud, J. K. Kochi, *J. Am. Chem. Soc.* **1986**, *108*, 2309–2320.

[6] R. Irie, K. Noda, Y. Ito, N. Matsumoto, T. Katsuki, *Tetrahedron Lett.* **1990**, *21*, 7345–7348.

[7] [7a] W. Zhang, J. L. Loebach, S. R. Wilson, E. N. Jacobsen, *J. Am. Chem. Soc.* **1990**, *112*, 2801–2803. [7b] E. N. Jacobsen, W. Zhang, M. L. Güler, *J. Am. Chem. Soc.* **1991**, *113*, 6703–6704. [7c] E. N. Jacobsen, W. Zhang, A. R. Muci, J. R. Ecker, L. Deng, *J. Am. Chem. Soc.* **1991**, *113*, 7063–7064.

[8] [8a] T. Katsuki, *Coord. Chem. Rev.* **1995**, *140*, 189–214. [8b] T. Katsuki, *J. Mol. Cat. A* **1996**, *113*, 87–107.

[9] [9a] E. N. Jacobsen, in *Catalytic Asymmetric Synthesis* (Ed.: I. Ojima,), VCH Verlagsgesellschaft, Weinheim, **1993**, chapter 4.2. [9b] E. N. Jacobsen, in *Comprehensive Organometallic Chemistry II, Vol. 12* (Eds: G. Wilkinson, F. G. A. Stone, E. W. Abel, L. S. Hegedus), Pergamon, New York, **1995**, chapter 11.1.

[10] J. F. Larrow, E. N. Jacobsen, Y. Gao, Y. Hong, X. Nie, C. M. Zepp, *J. Org. Chem.* **1994**, *59*, 1939–1942.

[11] C. E. Song, E. J. Roh, *Chem. Commun.* **2000**, 837–838.

[12] C. T. Dalton, K. M. Ryan, V. M. Wall, C. Bousquet, D. G. Gilheany, *Top. Catal.* **1998**, *5*, 75–91.

[13] D. Feichtinger, D. A. Plattner, *Angew. Chem.* **1997**, *109*, 1796; *Angew. Chem. Int. Ed. Engl.* **1997**, *36*, 1718–1719.

[14] D. Feichtinger, D. A. Plattner, *J. Chem. Soc., Perkin Trans. 2* **2000**, 1023–1028.

[15] [15a] J. T. Groves, J. Lee, S. S. Marla, *J. Am. Chem. Soc.* **1997**, *119*, 6269–6273. [15b] N. Jin, J. T. Groves, *J. Am. Chem. Soc.* **1999**, *121*, 2923–2924.

[16] T. Linker, *Angew. Chem.* **1997**, *109*, 2150–2152; *Angew. Chem. Int. Ed. Engl.* **1997**, *36*, 2060–2062.

[17] N. S. Finney, P. J. Pospisil, S. Chang, M. Palucki, R. G. Konsler, K. B. Hansen, E. N. Jacobsen, *Angew. Chem.* **1997**, *109*, 1798; *Angew. Chem. Int. Ed. Engl.* **1997**, *36*, 1720–1723.

[18] C. Linde, M. Arnold, P.-O. Norrby, B. Åckermark, *Angew. Chem.* **1997**, *109*, 1802–1803; *Angew. Chem. Int. Ed. Engl.* **1997**, *36*, 1723–1725.

[19] M. Palucki, N. S. Finney, P. J. Pospisil, M. L Güler, T. Ishida, E. N. Jacobsen, *J. Am. Chem. Soc.* **1998**, *120*, 948–954.

[20] W. Adam, R. T. Fell, V. R. Stegemann, C. R. Saha-Möller, *J. Am. Chem. Soc.* **1998**, *120*, 708–714.

[21] W. Adam, T. Wirth, *Acc. Chem. Res.* **1999**, *32*, 703–710.

[22] W. Adam, V. R. Stegemann, C. R. Saha-Möller, *J. Am. Chem. Soc.* **1999**, *121*, 1879–1882.

[23] T. Hamada, T. Fukuda, H. Imanishi, T. Katsuki, *Tetrahedron* **1996**, *52*, 515–530.

[24] T. Strassner, K. N. Houk, *Org. Lett.* **1999**, *1*, 419–421.

[25] [25a] A. D. Becke, *J. Chem. Phys.* **1993**, *98* 1372–1377. [25b] A. D. Becke, *J. Chem. Phys.* **1993**, *98* 5648–5652.

[26] P. J. Stephens, F. J. Devlin, C. F. Chabalowski, M. J. Frisch, *J. Phys. Chem.* **1994**, *98*; 11623–11627.

[27] C. Linde, B. Åckermark, P.-O. Norrby, M. Svensson, *J. Am. Chem. Soc.* **1999**, *121*, 5083–5084.

[28] S. Shaik, M. Filatov, D. Schröder, H. Schwarz, *Chem. Eur. J.* **1998**, *4*, 193–199.

[29] D. Schröder, S. Shaik, H. Schwarz, *Acc. Chem. Res.* **2000**, *33*, 139–145.

[30] D. Plattner, *Angew. Chem.* **1999**, *111*, 86–90; *Angew. Chem. Int. Ed.* **1999**, *38*, 82–86.

[31] L. Cavallo, H. Jacobsen, *Angew. Chem.* **2000**, *112*, 602–604; *Angew. Chem. Int. Ed.* **2000**, *39*, 589–592.

[32] [32a] A. D. Becke, *Phys. Rev. A* **1988**, *38*, 3098–3100. [32b] J. P. Perdew, *Phys. Rev. B* **1986**, *33*, 8822–8824.

[33] D. A. Plattner, D. Feichtinger, J. El-Bahraoui, O. Wiest, *Int. J. Mass Spectrom.* **2000**, *195/196*, 351–362.

[34] [34a] T. Ziegler, *Chem. Rev.* **1991**, *91*, 651–667. [34b] T. Ziegler, *Can. J. Chem.* **1995**, *73*, 743–761.

[35] L. A. Eriksson, L. G. M. Pettersson, P. E. M. Siegbahn, U. Wahlgren, *J. Chem. Phys.* **1995**, *102*, 872–878.

[36] [36a] S. Yanagisawa, T. Tsuneda, K. Hirao, *J. Chem. Phys.* **2000**,

112, 545−553. [36b] S. Yanagisawa, T. Tsuneda, K. Hirao, *J. Comput. Chem.* **2001**, *22*, 1995−2009.
[37] C. J. Barden, J. C. Rienstra-Kiracofe, H. F. Schaefer, *J. Chem. Phys.* **2000**, *113*, 690−700.
[38] P. E. M. Siegbahn, M. R. A. Blomberg, *Chem. Rev.* **2000**, *100*, 421−437.
[39] [39a] X. G. Zhao, W. H. Richardson, J.-L. Chen, J. Li, L. Noodleman, H.-L. Tsai, D. N. Hendrickson, *Inorg. Chem.* **1997**, *36*, 1198−1217. [39b] J. Li, C. L. Fisher, R. Konecny, D. Bashford, L. Noodleman, *Inorg. Chem.* **1999**, *38*, 929−939.
[40] Y. G. Abashkin, J. R. Collins, S. K. Burt, *Inorg. Chem.* **2001**, *40*, 4040−4048.
[41] T. A. Albright, J. K. Burdett, M.-H. Whangboo, *Orbital Interactions in Chemistry*; John Wiley & Sons: New York, **1985**, chapter 16.4.
[42] [42a] K. P. Bryliakov, D. E. Babushkin, E. P. Talsi, *Mendeleev Commun.* **1999**, 29−32. [42b] K. P. Bryliakov, D. E. Babushkin, E. P. Talsi, *Mendeleev Commun.* **2000**, 1−2A. [42c] K. P Bryliakov, D. E. Babushkin, E. P. Talsi, *J. Mol. Cat. A* **2000**, *158*, 19−35.
[43] K. A. Campbell, M. R. Lashley, J. K. Wyatt, M. H. Nantz, R. D. Britt, *J. Am. Chem. Soc.* **2001**, *123*, 5710−5719.
[44] F. B. van Duijneveldt, J. C. G. M. van Duijneveldt-van de Rijdt, J. H. van Lenthe, *Chem. Rev.* **1994**, *94*, 1873−1895.
[45] H. Jacobsen, L. Cavallo, *Chem. Eur. J.* **2001**, *7*, 800−807.
[46] P. Margl, L. Deng, T. Ziegler, *Organometallics* **1998**, *17*, 933−946.
[47] J. El-Bahraoui, O. Wiest, D. Feichtinger, D. A. Plattner, *Angew. Chem.* **2001**, *113*, 2131−2134; *Angew. Chem. Int. Ed.* **2001**, *40*, 2073−2076.
[48] P.-O. Norrby, C. Linde, B. Åckermark, *J. Am. Chem. Soc.* **1995**, *117*, 11035−11036.
[49] D. Feichtinger, D. A. Plattner, *Chem. Eur. J.* **2001**, *7*, 591−599.
[50] [50a] P. Gisdakis, S. Antonczak, Köstlmeier, W. A. Herrmann, N. Rösch, *Angew. Chem.* **1998**, *110*, 2333−2336; *Angew. Chem. Int. Ed.* **1998**, *37*, 2211−2214. [50b] I. V. Yudanov, C. Di Valentin, P. Gisdakis P, N. Rösch, *J. Mol. Cat. A* **2000**, *158*, 189−197. [50c] P. Gisdakis, I. V. Yudanov, N. Rösch, *Inorg. Chem.* **2001**, *40*, 3755−3765.
[51] [51a] D. V. Deubel, G. Frenking, H. M. Senn, J. Sundermeyer, *Chem. Commun.* **2000**, 2469−2470. [51b] D. V. Deubel, J. Sundermeyer, G. Frenking, *Inorg. Chem.* **2000**, *39*, 2314−2320. [51c] D. V. Deubel, J. Sundermeyer, G. Frenking, *J. Am. Chem. Soc.* **2000**, *122*, 10101−10108. [51d] D. V. Deubel, J. Sundermeyer, G. Frenking, *Eur. J. Inorg. Chem.* **2001**, 1819−1827.
[52] W. Adam, C. Mock-Knoblauch, C. R. Saha-Möller, M. Herderich, *J. Am. Chem. Soc.* **2000**, *122*, 9685−9691.
[53] [53a] T. Ikeno, I. Iwakura, T. Yamada, *Bull. Chem. Soc. Jpn.* **2001**, *74*, 2151−2160. [53b] T. Ikeno, I. Iwakura, S. Yabushita, T. Yamada, *Org. Lett.* **2002**, *4*, 517−520.
[54] C. Linde, N. Koliaï, P.-O. Norrby, B. Åckermark, *Chem. Eur. J.* **2002**, *8*, 2568−2573.
[55] W. Adam, K. J. Roschmann, C. Sahu-Möller, D. Seebach, *J. Am. Chem. Soc.* **2002**, *124*, 5068−5073.
[56] C. Fonseca Guerra, J. G. Snijders, G. te Velde, E. J. Baerends, *Theor. Chem. Acc.* **1998**, *99*, 391−403.
[57] S. H. Vosko, L. Wilk, M. Nusair, *Can. J. Phys.* **1980**, *58*, 1200−1211.
[58] E. J. Baerends, D. E. Ellis, P. Ros, *Chem. Phys.* **1973**, *2*, 41−51.
[59] G. te Velde, E. J. Baerends, *J. Comput. Phys.* **1992**, *99*, 84−98.
[60] L. Versluis, T. Ziegler, *J. Chem. Phys.* **1988**, *88*, 322−328.
[61] [61a] J. C. W. Lohrenz, T. Woo, T. Ziegler, *J. Am. Chem. Soc.* **1995**, *117*, 12793−12800. [61b] L. Cavallo, *J. Am. Chem. Soc.* **1999**, *121*, 4238−4241. [61c] M. Cheong, R. Schmid, T. Ziegler, *Organometallics* **2000**, *19*, 1973−1982. [61d] M. Solà, L. Cavallo, *J. Am. Chem. Soc.* **2001**, *123*, 12294−12302.

Received June 6, 2002
[I02301]